



Corrosion inhibition of mild steel in acidic solution by cow dung extract as an eco-friendly inhibitor

S. J. Olusegun^{*1}, O. O. Oluwasina³, K. K. Alaneme^{1,2}, P. A. Olubambi⁴

¹Department of Metallurgical and Materials Engineering, Federal University of Technology, Akure, Nigeria

²Department of Mining and Metallurgical Engineering, University of Namibia, Ongwediva Engineering Campus, Ongwediva, Namibia

³Department of Chemistry, Federal University of Technology, Akure, Nigeria

⁴Department of Chemical and Metallurgical Engineering, Tshwane University of Technology, Pretoria, South Africa

Received 25 Jan 2015, Revised 10Jan 2016, Accepted 20Jan 2016

*Corresponding author: E-mail: arikawedy@yahoo.com; sjolusegun@futa.edu.ng; Tel: (+234-8035116189)

Abstract

The anti corrosion potential of cow dung was assessed using weight loss, Electrochemical techniques, Fourier transform infrared spectroscopy (FTIR), Scanning electron microscopy (SEM) along with Energy dispersive spectroscopy (EDS), and Atomic absorption spectroscopy (AAS). The results show that cow dung extract (CDE) possesses good inhibition properties. The inhibition efficiency was found to increase with concentration but decrease with temperature. The highest inhibition efficiency obtained was 91% at 303K. Potentiodynamic polarization result suggests that CDE functioned as a mixed-type inhibitor. The AAS analysis shows that the concentration of Fe^{2+} in the electrolyte decreases with increase in the extract concentration. The adsorption of extract on the metal surface followed both Langmuir and Freundlich adsorption isotherms though Langmuir model better explained the adsorption process involved.

Keywords: corrosion inhibition, mild steel, cow dung, HCl, adsorption,

Introduction

Degradation of steel based material systems by corrosion is a common feature in industries where processes such as pickling, descaling, cleaning, oil well acidization are carried out [1]. Acids which are frequently utilized for these processes easily react with steel to form unprotective (or non-protective)oxides which result in gradual steel material loss and strength impoverishment [2]. An enormous corpus of literatures on strategies of controlling corrosion are available but work still persists in this area as researchers are on the look for more cost effective, technically efficient and environmentally friendly corrosion control strategies. This quest is motivated by the huge cost spent annually on corrosion control and monitoring technologies.

The use of plant source green inhibitors has been very promising in the search for more cost effective and technically efficient substances for corrosion control. Among plants that there exist documented research evidence of their effectiveness as inhibitors are *Justicia gendarussa* [3] *Phyllanthus amarus* [4] *Jatropha Curcas* [5] *Tithonia Diversifolia* [6] *Curcuma Longa* [7] *Rice Husk* [8] *Treculia Africana*, [9] *Atropa Belladonn* [10] *Eichhornia Crassipes*[11] *Pavetta Indica* [12] *Vernonia amygdalina* [13] *Eucalyptus citriodora* [14] *Hunterial Umbellata* [15]. There are also many other plant sources whose inhibition properties are still under investigation.

Despite the success of plant based green inhibitors, there have been a number of concerns raised about their sustainability in the long term particularly plant sources that have other competing domestic, medicinal and industrial uses [16]. It is thus timely for exploration of other potential sources of green inhibitors outside the use of plants.

The use of animal dung as potential source of developing corrosion inhibitor is currently under explored. Our team had worked on chitosan extracted from *Archachatina marginata* shells as corrosion inhibitor for mild steel in acidic medium with very promising results obtained [17]. The potentials of cow dung as corrosion inhibitor of steel in an acidic environment is the focus of this paper. The choice of cow dung was propelled by results obtained from its characterization which show the presence of OH among others. Organic compounds containing nitrogen, sulfur, oxygen, and heterocyclic compounds with a polar functional group and a conjugated double bond have been reported to inhibit mild steel corrosion [18]. The present study assessed the inhibition efficiency of cow dung in hydrochloric acid solutions. The focus on cow dung was influenced by its utilization as methanol, biogas and biochar production [19-22]. There is currently no report available in recognized peer reviewed article databases on the corrosion inhibition of cow dung.

2. Materials and methods

2.1 Materials

The plain carbon steel used for the study is mild steel of the following composition (wt. %: 0.0061% P; 0.82% M; 0.133% C; 0.08% Cr; 98.3% Fe). The steel was mechanically cut to coupons of dimension 20 x 10 cm, and then polished using silicon carbide paper of different grades. Analar grade HCl supplied by BDH laboratory and distilled water were used for the preparation of the electrolyte. Cow dung used was obtained as being excreted by local cow called Bokolo species from Akure cow market along Ado Road. This was sun dried to reduce the moisture content and then dried in oven at 105°C to constant moisture content of 10.30%.

2.2 Inhibitor preparation

The dry cow dung used was pulverized. 10g of the pulverized dung was added to 100ml of 1M HCl. The mixture was place in a water bath at 90°C for 3 hours. The mixtures was cooled and filtered. From the filtrate, 0.1, 0.5, 1.0, 1.5 and 2.0% v/v was prepared as test solution in 1M HCl.

2.3 Extract characterization

Cow dung extract was characterized using FTIR (Fourier transform infrared spectroscopy) and SEM-EDS (Scanning electron microscopy and Energy dispersive spectroscopy).

2.4. Chemical analysis

Phytochemical analysis of the extract of cow dung was carried out according to the method reported by Charu et al., [23]. Frothing test was used for the identification of saponin. Ferric chloride was used for the identification of tannin. Cardiac glycosides were tested using the Legal, Lieberman, Salkowski and Keller-killiani's test. Ammonia solution and conc. H₂SO₄ were used for the identification of flavonoid.

2.5 Gravimetric measurement

The polished and pre-weighed mild steel coupons were immersed in 250 ml beaker containing 100 ml test solution, maintained at different temperatures in the range of 303–333 K for 4 h. After 4 h immersion, the specimens were taken from the solution, dried in acetone and then weighed. The weight loss, (in milligrams), was taken as the difference in the weight of the mild steel coupons before and after immersion in different test solutions. The weight loss was used to calculate the corrosion rate (CR) and the inhibition efficiency (IE) using equations 1 and 2

$$CR \text{ (mgh}^{-1}\text{)} = \frac{\Delta W}{AT} \quad 1$$

Where CR is corrosion rate, ΔW is weight loss, A is the area of the coupon and T is time in hour

$$I.E\% = \left(1 - \frac{CR_{inh}}{CR_{blank}}\right) \times 100 \quad 2$$

Where, CR_{inh} and CR_{blank} correspond to the corrosion rates in the presence and absence of inhibitor respectively. I.E is the inhibition efficiency.

2.6 Potentiodynamic polarization measurement

The electrochemical experiments were carried out using AUTOLAB PGSTAT 302N instrument, piloted by Nova software. The experiments were performed using a three-electrode corrosion cell set-up comprising of mild steel as the working electrode, saturated silver/silver chloride as reference electrode, and graphite rod as counter electrode. The test electrolyte was 1M solution of HCl. The working electrode was immersed in a test solution for one hour until a stable open circuit potential was attained. The working electrodes were prepared by attaching an insulated copper wire to one face of the sample using an aluminum conducting tape, and cold mounting it in resin.

Potentiodynamic polarization measurements were carried out using a scan rate of 1.0 mV/s at a potential range of -200mV to + 1500mV with respect to OCP. After each experiment, the electrolyte and the test samples were replaced. The linear Tafel segments of the anodic and cathodic curves were extrapolated to obtain corrosion potential (E_{corr}) and corrosion current densities (I_{corr}).

2.7 Atomic Adsorption Spectroscopy (AAS) Analysis

Atomic adsorption analysis was conducted by using atomic adsorption spectrometer model AAS Buck Scientific 210 VGP to determine the concentration of iron (II) ions in 1 M hydrochloric acid after gravimetric measurements. All samples containing iron ions were diluted with distilled water to ensure that the concentrations of metal ions are within the range of the calibration curve.

2.8 Fourier Transform Infrared Spectroscopy (FTIR) Analysis

Finely powdered (iron filing) mild steel specimen was immersed in a solution of hydrochloric acid containing the plants extract for 4 hours to form the adsorption product of Mild steel and the extract. FTIR spectrum was recorded for the extracts and the adsorption product. These spectra were recorded in a Perkin-Elmer-1600 spectrophotometer using KBr pellet.

2.9 Scanning Electron Microscopy and Energy dispersive spectroscopy (SEM-EDS) Analysis

The surface morphology of the mild steel before and after immersion were examined with scanning electron microscopy equipped with energy dispersive spectroscopy to analyze the elements in the surface, using a JSM 7600F Jeol ultra-high resolution field emission gun scanning electron microscope (FEG-SEM).

3. Results and discussion

3.1 Phytochemical screening

Phytochemical constituents of the extracts as presented in Table 1, shows the presence of tannins, saponins et cetera. The presence of these compounds promote the inhibition of mild steel in the aggressive medium.

Table 1 Phytochemical constituents of CDE

Phytochemical constituents	Saponins	Tannins	Flavonoids
Cow dung extract	+	+	+

Key (+) = present in small amount

3.2 Cow dung characterization

Figure 1 displays the SEM and EDS spectra of cow dung. The EDS line-analyses were performed on the cross-sections to reveal the corresponding elemental distribution. The main constituents within the layers were showing a non-uniform spectrum composed of C, O, Si and P. FTIR spectroscopy has been widely employed as an effective tool to identify the functional group present in a particular substance. Presented in Figure 2 is the FITR spectrum of cow dung that was used for the research work. The spectrum displayed different adsorption bands. There is a peak at 3438 cm^{-1} which is characteristics for the -OH stretching vibration. 2925 and 1646 cm^{-1}

¹ bands gave the characteristics of –CH and C=C stretching respectively. Most organic compounds that contain one or more heteroatoms such as oxygen, nitrogen or sulphur exhibit corrosion inhibition ability in acidic media. Organic molecules that have groups like -OH, -CHO, -COOH, -CN, -SCN, -CO, -NH₂, -SO₃, double or triple bonds or unpaired electrons, have been attested to interact easily with metals thereby leading to the protection of metals in aggressive medium [24].

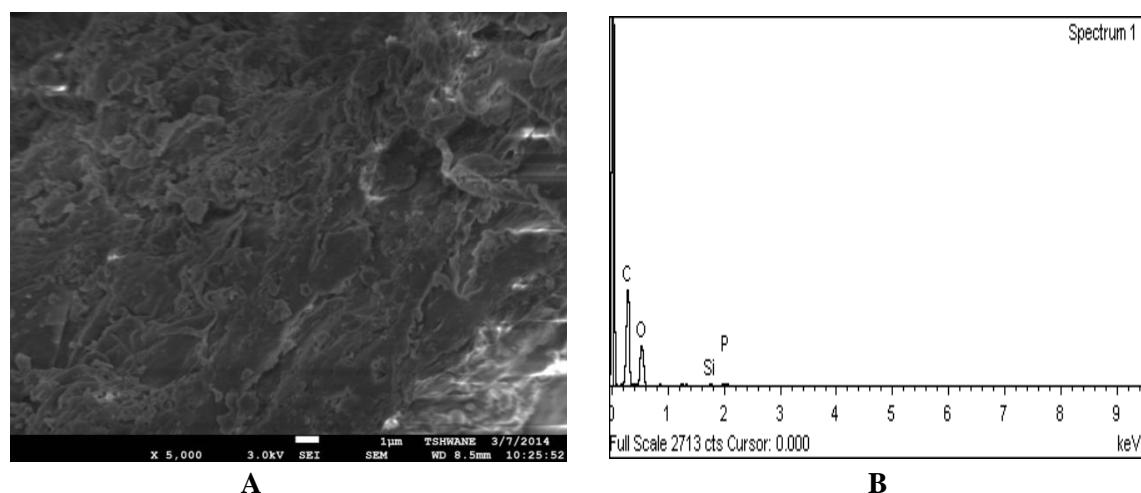


Figure 1. (a) SEM micrograph and (b) EDS spectra of cow dung

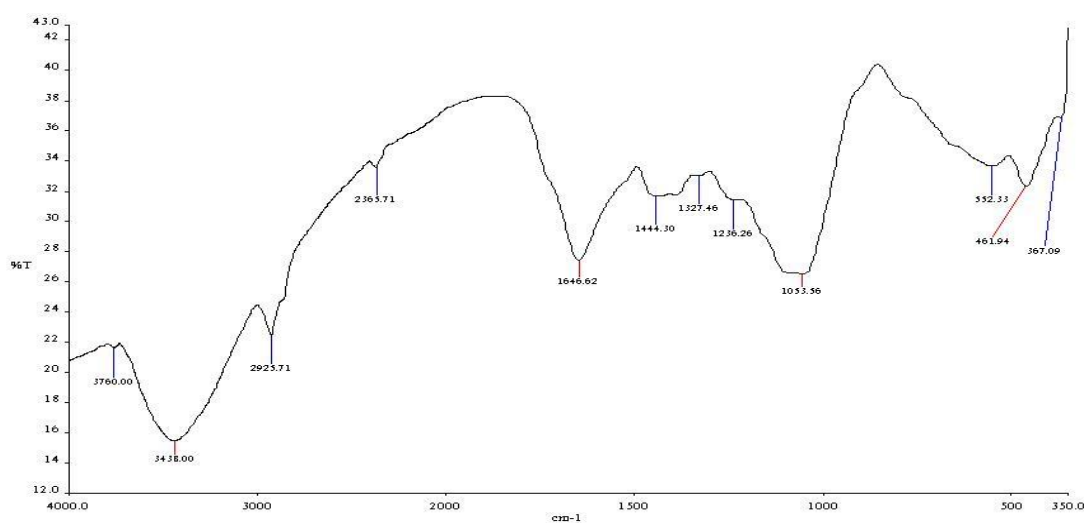


Figure 2. IR spectra of Cow dung

3.3 Mass loss measurement

The mass loss measurement of mild steel at room temperature immersed in absence and presence of different concentrations of cow dung extract (CDE) as a function of time is shown in Figure 3. The mass loss of mild steel increased with increased in exposure time, but decreased with the addition of CDE. The addition of the extract reduced the dissolution of mild steel in the solution. The presence of –OH in the extract would have facilitated the inhibition process of the steel. Fe²⁺ in the electrolyte coordinated with extract through the lone pairs of electron present in the oxygen thus leading to the formation of Fe²⁺-CDE complex on the metal surface [25]. The cow dung used was digested plant material from animal rumen and thus would contain elements found in plant material. The presence of tannins in the extract resulted to the formation of a passivating layer of tannates on the metallic surface [26]. The protective layer thus formed on the surface would have led to a decrease in the interaction between the metal and the corrosive environment thus created barriers for mass and charge transfer.

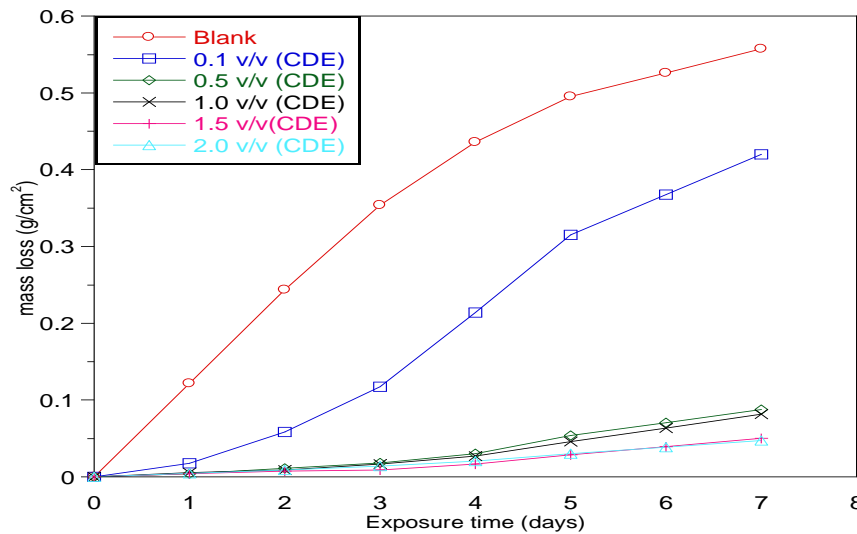


Figure 3: The variation of mass loss of mild steel in the absence and presence of CDE as a function of time

The AAS analysis results presented in Figure 4 (which shows the graph of the dissolution of Fe^{2+} in the electrolyte as function of the extract concentration), supports the mass loss trends reported in Figure 3. It is seen that there is a steady decrease in the concentration of Fe^{2+} in the electrolyte as the concentration of cow dung extract increases. This indicates that the adsorption of the extract on the metal surface reduced the oxidation of iron atom Fe to Fe^{2+} . It should be noted that the mitigation of corrosion of the steel substrates apart from prolonging the life span of the substrate also reduces the amount of toxic iron (II) dissolved from the components into the environment. This helps reduce the resources invested in the treatment of the effluents from acid and cleaning industries.

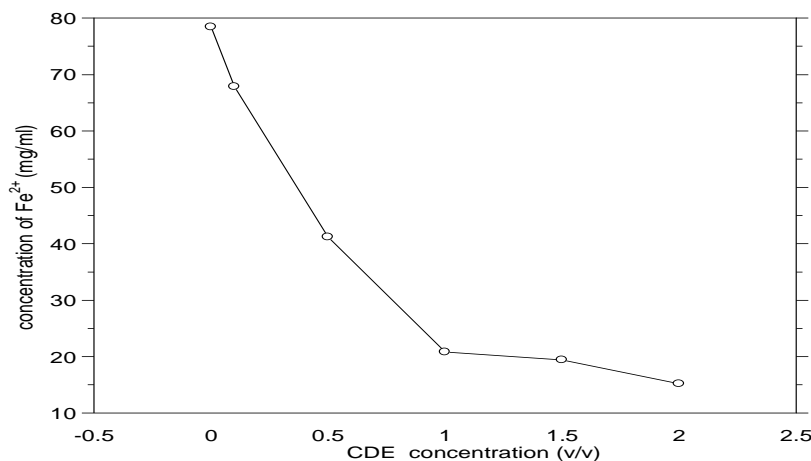


Figure 4: Plot of the concentrations of iron (II) ions in 1 M hydrochloric acid after gravimetric measurements

3.4 Electrochemical measurement

Figure 5 shows the potentiodynamic polarization curves of corrosion inhibition of mild steel in 1M HCl in absence and presence of different concentrations of CDE. It was observed from the Figure that addition of CDE affect both anodic and cathodic polarization curves suggesting that the CDE could be classified as mixed-type inhibitor (reduced the mild steel dissolution as well as hydrogen evolution). This could be as a result of the adsorption of the inhibitor molecules on the surface of the metal (working electrode). Table 2 shows the electrochemical kinetics parameters; corrosion potential (E_{corr}), anodic Tafel slope (β_a), cathodic slope (β_c) and corrosion current density (I_{corr}) were obtained by extrapolation of the Tafel lines. It was clearly seen from the table that the corrosion current density (I_{corr}) values decreased as the concentration of CDE increased. This shows that the addition CDE reduced the metal dissolution process.

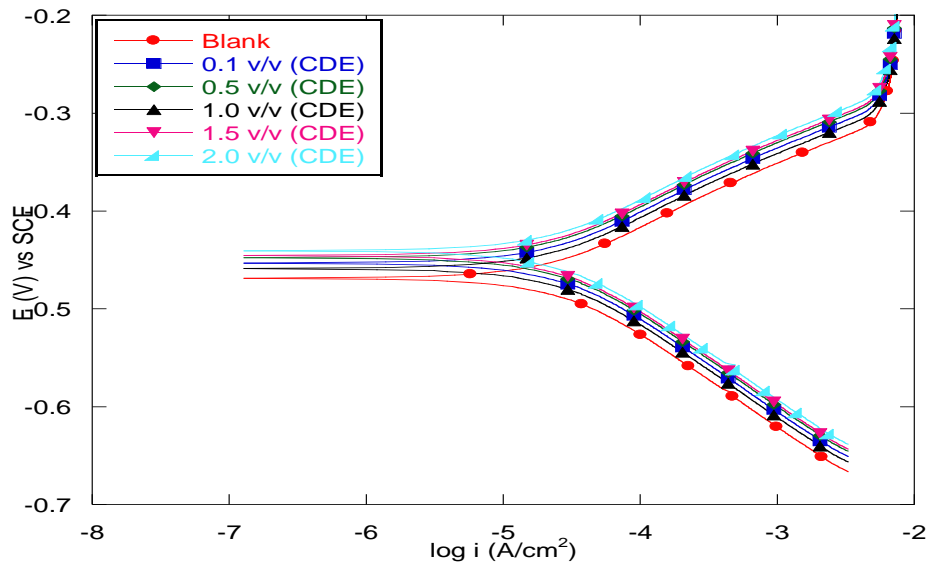


Figure 5: Potentiodynamic polarization curves for the mild steel in the absence and presence CDE

Table 2: Electrochemical polarization parameters for mild steel in 1.0 M HCL at different concentrations of corrosion inhibitors.

Inhibitor concentration (% v/v)	-E _{corr} (mv/SCE)	I _{corr} (μ A/cm ²)	β_a (mV/dec)	β_c (mV/dec)	IE %
Blank	463	122	92	92	-
0.1	411	77	67	19	36
0.5	446	58	97	91	52
1.0	452	38	97	12	68
1.5	443	32	86	78	73
2.0	439	19	77	71	84

3.5 Effects of temperature on inhibition efficiency and corrosion rate.

The variation of inhibition efficiency with concentration of the CDE at different temperatures is presented in Figure 6.

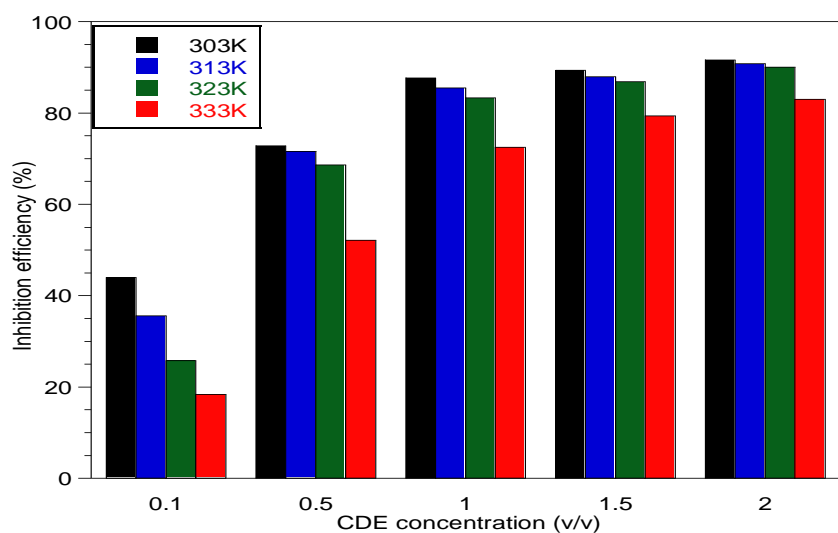


Figure 6. Variation of inhibition efficiency of CDE with temperature

It is observed that the inhibition efficiency increases with increase in CDE concentration but decreases with increase in temperature. Ben Hmamou *et al.*, [27] explained that adsorption and desorption of inhibitor molecules occurs steadily at the metal surface and that equilibrium will exist between these two processes at a particular temperature. With the increase of temperature, the equilibrium between adsorption and desorption process is shifted leading to a higher desorption rate than adsorption until equilibrium is again established at a different values of equilibrium constant [27].

Decrease in inhibition efficiency at high temperature could also be as a result of the active compounds in the extract to thermolabile that is, high temperature degradation of active compounds. In view of this, the decrease in inhibition with respect to increase in temperature occurs because at higher temperatures the oxide films that were formed on the metal surface would have desorbed. This implies that desorption/solubility of the films oxides exposed the metals to the aggressive environment.

The values of corrosion rate at different temperature are summarized in Table 3. From the Table it is clear that corrosion rate increases with increase in temperature. This happened to be the case because as the temperature increases the average kinetic energy of the reactant molecules increases and thereby increasing the rate of the reaction [28].

Table 3. Calculated values of corrosion rate for mild steel in 1M HCl in the absence and presence of CDE at 303–333K.

Acid medium	CDE concentration (% v/v)	Corrosion rate (mg cm ⁻² h ⁻¹)			
		303K	313K	323K	333k
1M HCl	Blank	11.27	16.86	27.99	45.47
	0.1	6.31	10.86	20.77	37.1
	0.5	3.06	4.79	8.78	21.77
	1.0	1.39	2.45	4.67	12.49
	1.5	1.19	2.03	3.69	9.39
	2.0	0.94	1.55	2.79	7.74

The corrosion rate values obtained in Table 3 were used to evaluate the activation energy. From Arrhenius equation the plot of log CR as a function of 1/T both in the absence and presence of CDE is linear as shown in Figure 7:

$$\log CR = \log A - \frac{E_a}{2.303RT} \quad 3$$

Where CR is the corrosion rate, E_a is the apparent activation energy, R is the molar gas constant, T is the absolute temperature and A is the frequency factor, T is the absolute temperature.

The values of activation energy obtained from the slope are presented in Table 4 the E_a values obtained in the presence of the extract are more than in the absence. This indicates that the CDE, being a negative catalyst, inhibit the mild steel sample by increasing the energy barrier for the dissolution of the metal into the electrolyte. Increase in activation energy values in the presence of the extract with respect to the absence as being attributed to physical adsorption mechanism while the opposite is chemisorptions [29].

The corrosion rates values obtained at different temperatures in the presence and absence of CDE were also used to evaluate the change in enthalpy and entropy of metal dissolution using the transition state equation

$$\log \frac{CR}{T} = \left[\log \left(\frac{R}{nh} \right) + \frac{\Delta S_a}{2.303R} \right] - \frac{\Delta H_a}{2.303RT} \quad 4$$

Where CR is the corrosion rate, h is the Plank's constant (6.626176×10^{-34} J s), N is the Avogadro's number (6.02252×10^{23} mol⁻¹), R is the universal gas constant and T is the absolute temperature. Figure 8 shows the plot log CR/T vs. 1/T which is linear, with a slope of ($-\Delta H/2.303R$) and an intercept of ($\log(R/nh) + \Delta S/2.303R$) from which the values of ΔH_a and ΔS_a are calculated and presented in Table 4

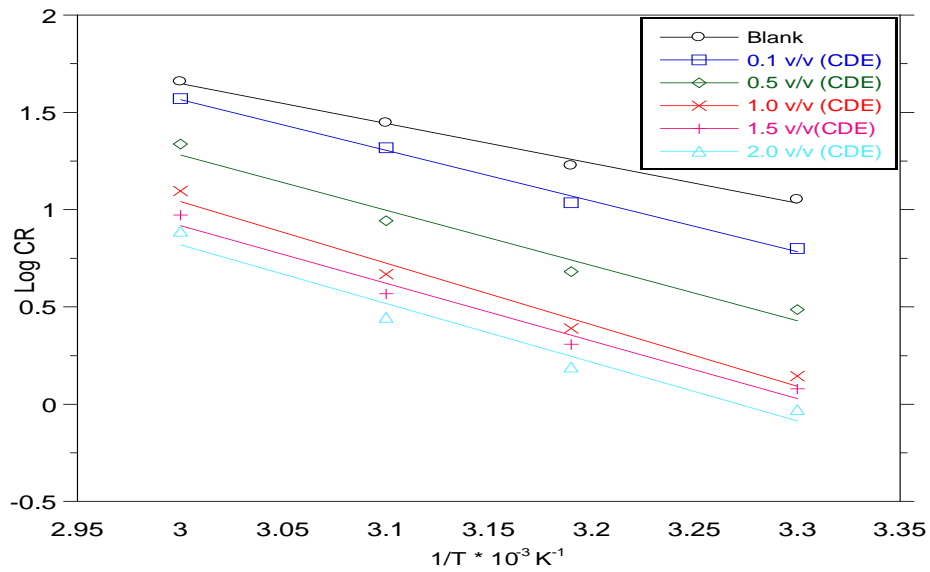


Figure 7. Arrhenius plot for mild steel corrosion in 1 M HCl in the absence and presence of CDE extract

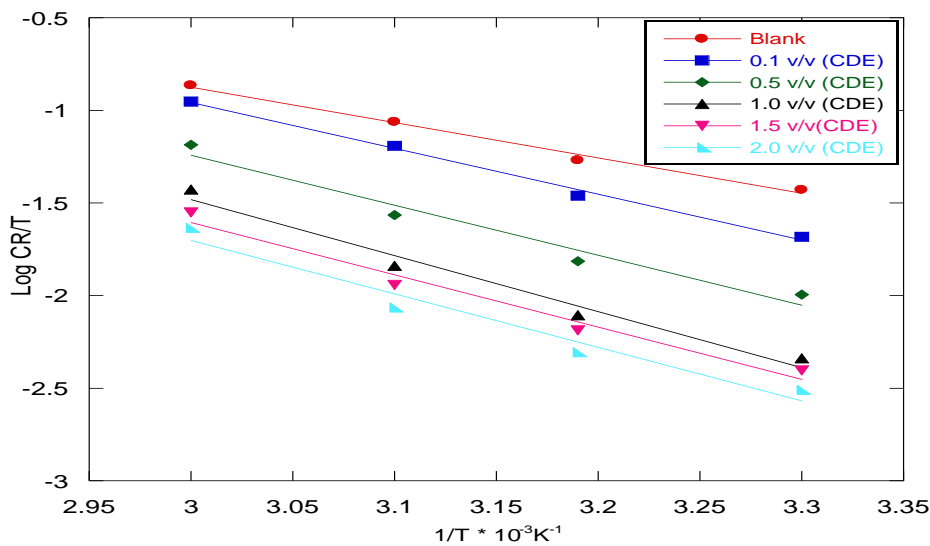


Figure 8. Transition state plot for mild steel corrosion in 1 M HCl in the absence and presence of CDE

Table 4. Activation energy, enthalpy and entropy parameters of the mild steel dissolution in 1 M HCl in the presence and absence of CDE at temperature range of 303–333K.

Acid medium	Concentration of CDE (% v/v)	Activation energy, E_a (kJ mol ⁻¹)	Enthalpy of activation, ΔH_a (kJ mol ⁻¹)	Entropy of activation, ΔS_a (J mol ⁻¹ K ⁻¹)
1 M HCl	Blank	39.28	36.64	-104.42
	0.1	49.95	47.31	-73.99
	0.5	54.29	51.65	-66.43
	1.0	60.54	57.91	-52.25
	1.5	56.71	54.07	-66.12
	2.0	57.87	55.23	-64.50

The results show that the enthalpy of activation values are all positive, which indicate the endothermic nature of the mild steel dissolution process in the electrolyte. The values obtained in the presence of CDE were higher than in the absence. This shows that the film oxide formed on the metal surface in the presence of CDE raised

the amount of the heat that will be needed for iron atom to oxidize to iron (II). Also, the entropies of activation were negative both in absence and presence of CDE. This shows that there is a decrease in the disordering process of the metal dissolution.

3.6 Adsorption isotherm

Inhibition efficiency is directly related to the level of the coverage of metal by the adsorbed inhibitors. The degree of surface coverage (Θ) that was used for the plot of the isotherms was calculated from the corrosion rate values.

$$\Theta = 1 - \frac{CR_{inh}}{CR_{blank}} \quad 5$$

The calculated surface coverage (Θ) was fitted into different isotherms, from the correlation coefficient obtained; Langmuir and Freundlich were found to be best applicable.

The Langmuir adsorption isotherm is applied to investigate the mechanism of the corrosion inhibition by the following equation:

$$\frac{C}{\theta} = \frac{1}{K_{ads}} + C \quad 6$$

Where C is the inhibitor concentration, θ is the surface coverage and k_{ads} is the adsorption equilibrium constant. The plot of C/θ against C is linear as shown in Figure 9 indicating that the adsorption of CDE on the surface of mild steel is consistent with Langmuir isotherm and the slopes obtained are unity. The correlation coefficient (R^2) of the adsorption isotherm data showed that Langmuir isotherm is fitted into the experiment with R^2 ranges from 0.9993 to 0.9998 for all the extracts and at different temperature

The values of correlation coefficient (R^2) and adsorption coefficient (K_{ads}) are shown in Table 5. The values of K_{ads} showed that adsorption coefficient decreases with increase in temperature. This indicates that the adsorption of CDE on the surface of mild steel is favorable at lower temperature and is in agreement with the results obtained for inhibition efficiency.

The data is also fitted into Freundlich adsorption model using the equation 7

$$\log \theta = \log K_f + \frac{1}{n} \log C \quad 7$$

Where K_f is Freundlich isotherm constant, n is adsorption intensity; C is the inhibitor concentration, Θ is the surface coverage.

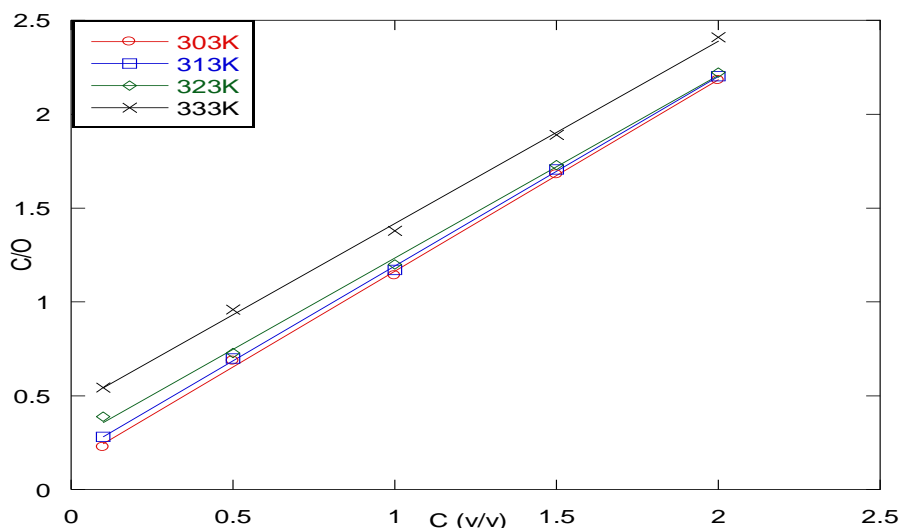


Figure 9. Langmuir adsorption isotherm plot for the adsorption of CDE on the surface of mild steel in 1 M hydrochloric acid

The plot of $\log \theta$ against $\log C$ is shown in Figure 10. The slope of the graph is $1/n$ where $\log K_f$ is the intercept. The constant K_f is an approximate indicator of adsorption capacity, while $1/n$ is a function of the strength of adsorption in the adsorption process [30, 31]. If $1/n = 1$ then the partition between the two phases are

independent of the concentration. If value of $1/n$ is below one it indicates a normal adsorption. On the other hand, $1/n$ being above one indicates cooperative adsorption [30, 32].

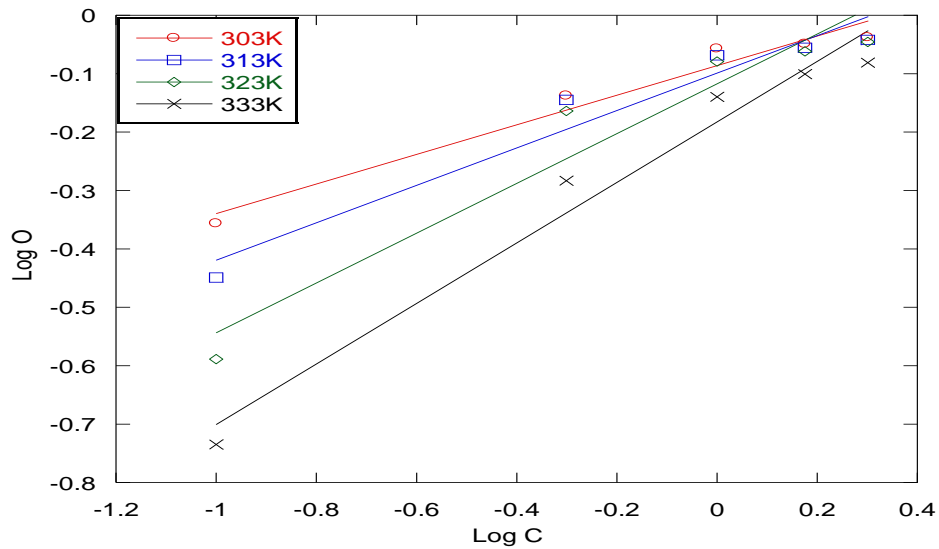


Figure 10. Freundlich adsorption isotherm plot for the adsorption of CDE on the surface of mild steel in 1 M hydrochloric acid

Table 5 Isotherms parameters the adsorption of CDE on the surface of mild steel

Temp.	Langmuir isotherm parameters			Freundlich isotherm parameters		
	K_{ads}	r^2	Slope	K_F	r^2	$\frac{1}{n}$
303K	7.03	0.9996	1.02	0.8207	0.9819	0.253
313K	5.52	0.9998	1.01	0.7959	0.9737	0.320
323K	3.84	0.9994	0.97	0.7629	0.9664	0.456
333K	2.25	0.9993	0.97	0.6571	0.9845	0.518

The value of $1/n$ for all the extract as shown in Table 5, is less than 1 indicating that adsorption of CDE that promote the inhibition of mild steel is a normal adsorption process and depended on concentration of the extracts. The correlation coefficient (R^2) ranges from 0.9664 to 0.9957. The values of K_f decrease as the temperature increase indicating that the adsorption capacity decreases with temperature. This is conjunction with what was obtained from Langmuir isotherm.

3.7 SEM and EDS analysis

The SEM photographs of the mild steel before and after immersion in hydrochloric acid in the absence and presence of CDE are presented in Figures 11 – 13

Surface analysis using scanning electron microscopy (SEM) provided more information on the inhibition of the extract on the surface of mild steel. The surface of the mild steel in the absence of inhibitor revealed that it has been seriously attacked by the acid with an evidence of pit formation, whereas the presence of the CDE reduced the level of attack on the metal surface.

The EDS (Energy dispersive spectroscopy) spectra are presented in Figures 11 – 13b. The higher signal of O in the absence of CDE as compare to the presence indicates that the Fe has reacted with O from the medium to form iron oxide as a corrosion product. The low content of oxygen in the EDS spectrum of the surface of mild

steel immersed in CDE may be as a result of the protective film on the surface of the metal which inhibited the formation of iron oxide. From the EDS evaluation of mild steel in the absence of inhibitor, it is clear that the upraising value of O is due to the formation of the ferrous hydroxide [33].

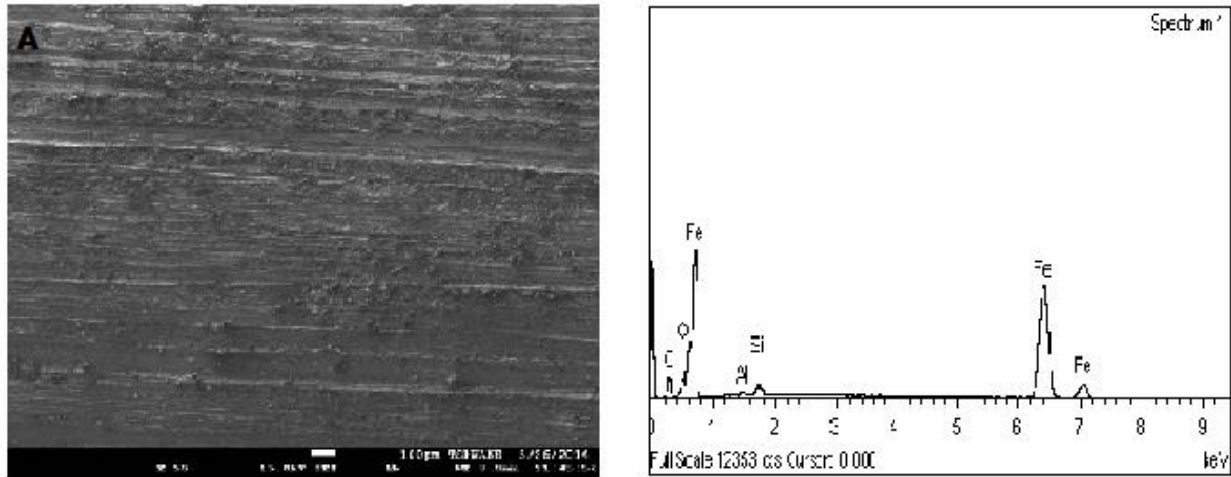


Figure 11. SEM micrograph and EDS spectra of plain mild steel

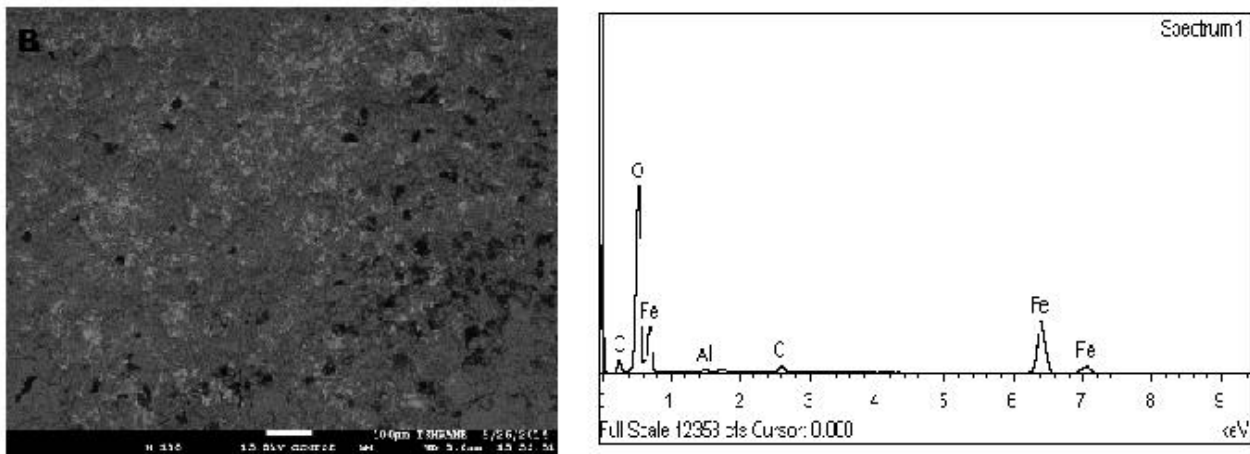


Figure 12. SEM micrograph and EDS spectra of steel immersed in hydrochloric acid in the absence of CDE

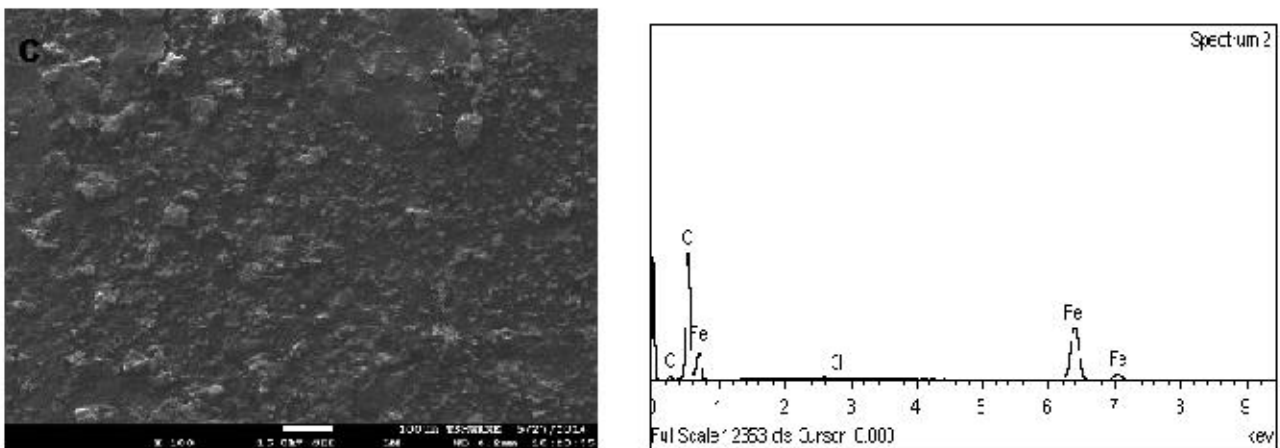


Figure 13. SEM micrograph and EDS spectra of mild steel immersed in HCl in the presence of CDE

Conclusion

The findings of the research work have proved that cow dung extract (CDE) is effective eco-friendly inhibitor. The inhibition efficiency increases with the increase in the concentration of the extracts but decreases as the temperature increases. Potentiodynamic polarization results indicate that CDE behave as mixed-type inhibitor. Physical adsorption mechanism is in conformation with the data obtained. Langmuir and Freundlich models were best fitted into the obtained results. The result of the SEM-EDS of the mild steel showed that the metal was well protected in the presence of CDE. The calculated activation energy values also conform to a physical adsorption mechanism.

References

1. Machnikova E., Whitmire K.H., and Hackerman N., *Electrochim. Acta* 53 (2008) 6024.
2. Soror T.Y. *Eur. Chem. Bull.* 4 (2013) 191-196
3. Satapathy A.K., Gunasekaran G, Sahoo S.C., Amit K, Rodrigues P.V., *Corros. Sci.* 51 (2009) 2848.
4. Okafor P.C., Ikpi ME, Uwah IE, Ebenso EE, Ekpe UJ, Umoren S.A., *Corros. Sci.* 50 (2008) 2310.
5. Olusegun S.J., Adeiza B.A., Ikeke K.I. and Bodunrin M.O., *JETEAS* 4 (2013)138.
6. Alaneme K.K., Olusegun S.J., *Leonardo J. Sci.* 20 (2012) 59.
7. Kairi N.I, Kassim J., *Int. J. Electrochem. Sci.* 8 (2013) 7138.
8. Alaneme K.K., Daramola Y.S., Olusegun S.J., Afolabi A.S. *Int J Electrochem Sci* 10 (2015) 3567.
9. Ejikeme P.M., Umana S.G., Onukwuli O.D., *Port. Electrochim. Acta* 30 (2012) 317.
10. Shalabi K., Abdallah Y.M., Hassan H.M., Fouda A.S., *Int. J. Electrochem. Sci.*, 9 (2014) 1468.
11. Oloruntoba D.T., Abbas J.A., Olusegun S.J., *Proceedings of 4th West Africa Built Environment Research (WABER), Abuja, July* (2012) 1140
12. Sheeja V.N., Subhashini S., *Chem. Sci. Trans*3 (2014)129.
13. Oluseyi Ajayi O. Olugbenga Omotosho A, Vincent O.I., *J. Mater. Environ. Sci.* 2 (2011) 186.
14. Ezeokonkwo M.A., Ukoha P.O., Nnaji N.J.N., *Int. J. Chem. Sci.*10 (2012) 1365.
15. Alaneme K.K., Olusegun SJ, Adelowo O.T., *Alexandria Eng. J.* (2015)
<http://dx.doi.org/10.1016/j.aej.2015.10.009>
16. Sangeetha M., Rajendran S., Muthumegala T.S., Krishnaveni A., *Zaštita Mater. Broj* 52 (2011) 3
17. Okoronkwo A.E., Olusegun S.J., Oluwasina O.O., *Anti Corros Mater. Meth.* 62 (2015) 13.
18. Noor A.E., *Mat. Chem. Phys.* 114 (2009) 531.
19. Ipeghan O.J., Ogedengbe V.E., *IJAEM*6 (2013) 91.
20. Olusegun A.A., Adefila S.S., *J. Environ and Earth Sci.* 2 (2012) 9
21. Utomo W.H., Nugroho W.H., Kusuma Z., *J. Basic. Appl. Sci. Res* 1 (2011)1680.
22. Tanimu J., Uyovbisere E.O., Lyocks S.W.J., Tanimu Y., *Greener J. Agric. Sci* 3 (2013) 371.
23. Charu A.C., Mehta S., Heena D., *Asian J. Chem* 24 (2012) 5903.
24. Zor S., Yazici B. *Turk J Chem* 23 (1999) 393.
25. Peter C.O., Ebenso E.E., Ekpe U.J., *Int. J. Electrochem. Sci.*5 (2010) 978.
26. Shyamala M, Kasthuri PK. A. *Int. J. Corros* (2011); doi:10.1155/2011/129647
27. Ben Hmamou D., Salghi R., Zarrouk A., Zarrok H., Hammouti B., Al-Deyab S.S., El Assyry A., Benchat N., Bouachrine M., *Int. J. Electrochem. Sci.* 8 (2013) 11526.
28. Olasehinde E.F., Olusegun S.J., Adesina A.S., Omogbehin S.A., Momoh-Yahayah H., *Nat Sci.* 11 (2013) 83.
29. Popova A., Sokolova E., Raicheva S., Christov M., *Corros. Sci.* 45 (2003) 33.
30. Dada A.O., Olalekan A.P., Olatunya A.M., Dada O., *IOSR J. App. Chem.*3 (2012) 38.
31. Voudrias E., Fytianos F., Bozani E., *Global Nest, The Int. J.*, 4 (2002)75.
32. Mohan S., Karthikeyan X., *J. Environ. Pollut.* 97 (1997) 183.
33. Hussin M.H., Mohd. J., *J. Phys. Sci.* 21 (2010) 1.

(2016) ; <http://www.jmaterenvironsci.com>